

Supporting Information

Preparation and structures of enantiomeric dinuclear zirconium and hafnium complexes containing two homochiral N atoms, and their catalytic property for polymerization of *rac*-lactide

Minggang Hu,^a Mei Wang,^{*a} Hongjun Zhu,^a Lu Zhang,^a Hui Zhang^b and Licheng Sun^{*a,c}

^a*State Key Laboratory of Fine Chemicals, DUT-KTH Joint Education and Research Centre on Molecular Devices, Dalian University of Technology, Dalian 116012, China. E-mail: symbueno@dlut.edu.cn*

^b*College of Chemistry and Chemical Engineering, Xiamen University, Xiamen 361005, China.*

^c*Department of Chemistry, Royal Institute of Technology, Stockholm 10044, Sweden.*

E-mail:lichengs@kth.se

Contents:

- Fig. S1 ^1H NMR spectrum of H_2L , page S4
- Fig. S2 ESI-Q-TOF mass spectra of **1**, page S5
- Fig. S3 ^1H NMR spectrum of **1**, page S5
- Fig. S4 ESI-Q-TOF mass spectra of **2**, page S6
- Fig. S5 ^1H NMR spectrum of **2**, page S6
- Fig. S6 ESI-Q-TOF mass spectra of **3**, page S7
- Fig. S7 ^1H NMR spectrum of **3**, page S7
- Crystal data and details of data collection for H_2L and L_2Zr , page S8
- Crystallographic data and of H_2L , page S9
- Fig. S8 Molecular structure of H_2L , page S9
- Crystallographic data of L_2Zr , page S10
- Crystallographic data of $\text{N}(\text{R})\text{N}(\text{R})\text{-2}$ and $\text{N}(\text{S})\text{N}(\text{S})\text{-2}$, pages S10 and S11
- Fig. S9 Framework structures of $\text{N}(\text{R})\text{N}(\text{R})\text{-2}$ and $\text{N}(\text{S})\text{N}(\text{S})\text{-2}$, page S11
- Crystallographic data of $\text{N}(\text{R})\text{N}(\text{R})\text{-3}$ and $\text{N}(\text{S})\text{N}(\text{S})\text{-3}$, pages S12 and S13
- Fig. S10 Methine region of homonuclear decoupled ^1H NMR spectra of isotactic-rich PLA made from *rac*-LA initiated by *rac*-**2** and *rac*-**3**, page S14
- Fig. S11 Polymerization of L-LA and microstructure analysis of PLLA, page S15

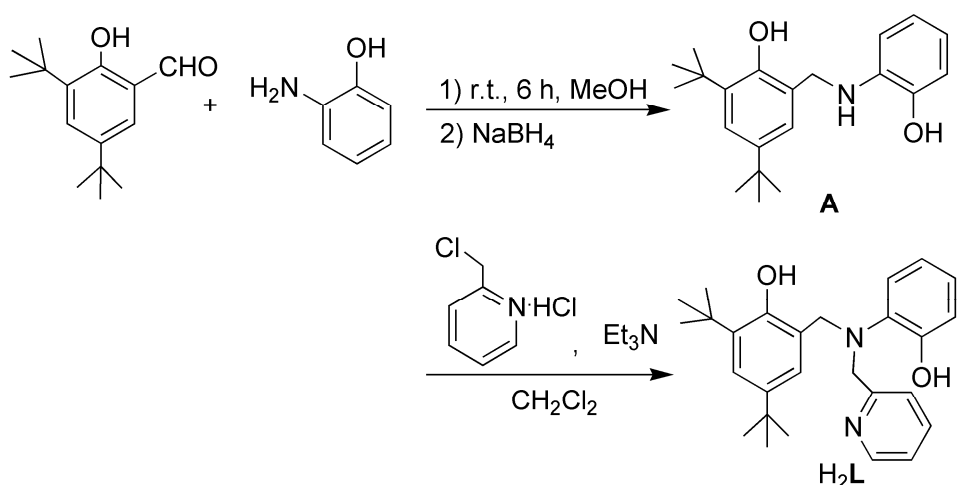
1. Preparation and spectroscopic characterization of H_2L and **1–3**

1.1 Preparation and spectroscopic characterization of H_2L

Unsymmetric ligand H_2L was prepared according to a modified procedure of the literature

(Scheme S1). A mixture of 3,5-di-*tert*-butyl-2-hydroxybenzaldehyde (4.68 g, 0.02 mol) and 2-aminophenol (2.18 g, 0.02 mol) was stirred in CH₃OH (50 mL) for 6 h, and then the solution was cooled to 0 °C before addition of NaBH₄ (0.76 g, 0.02 mol) in several portions. After 30 min, the solvent was removed and water (50 mL) was added. The mixture was neutralized with acetic acid. The off-white solid (**A**) was filtered, washed three times with water, and dried in vacuo. Yield: 6.1 g (93%).

To the suspension of 2-(chloromethyl)pyridine hydrochloride (1.4 g, 0.008 mol) in CH₂Cl₂ (20 mL), a solution of **A** (1.64 g, 0.005 mol) in CH₂Cl₂ (20 mL) was added dropwise at 0 °C, followed by dropwise addition of the CH₂Cl₂ solution (10 mL) of Et₃N (2.53 g, 0.025 mol) to the mixture. The stirring was maintained for 72 h at room temperature. The mixture was washed twice with water, and the organic layer was separated and dried with anhydrous MgSO₄. After removal of solvent, the residue was recrystallized from acetone/hexane. Ligand H₂L was obtained as an off-white crystalline solid (1.0 g, 48%). ¹H NMR (400 MHz, CDCl₃, 293 K): δ = 8.55 (d, 1H, Py), 7.39–6.61 (9H, Ph and Py), 4.35 (s, 2H, N-CH₂-Ph), 4.13 (s, 2H, N-CH₂-Py), 1.28 and 1.17 (2s, each for 9H, CH₃ of *tert*-Bu) (Fig. S1).



Scheme S1

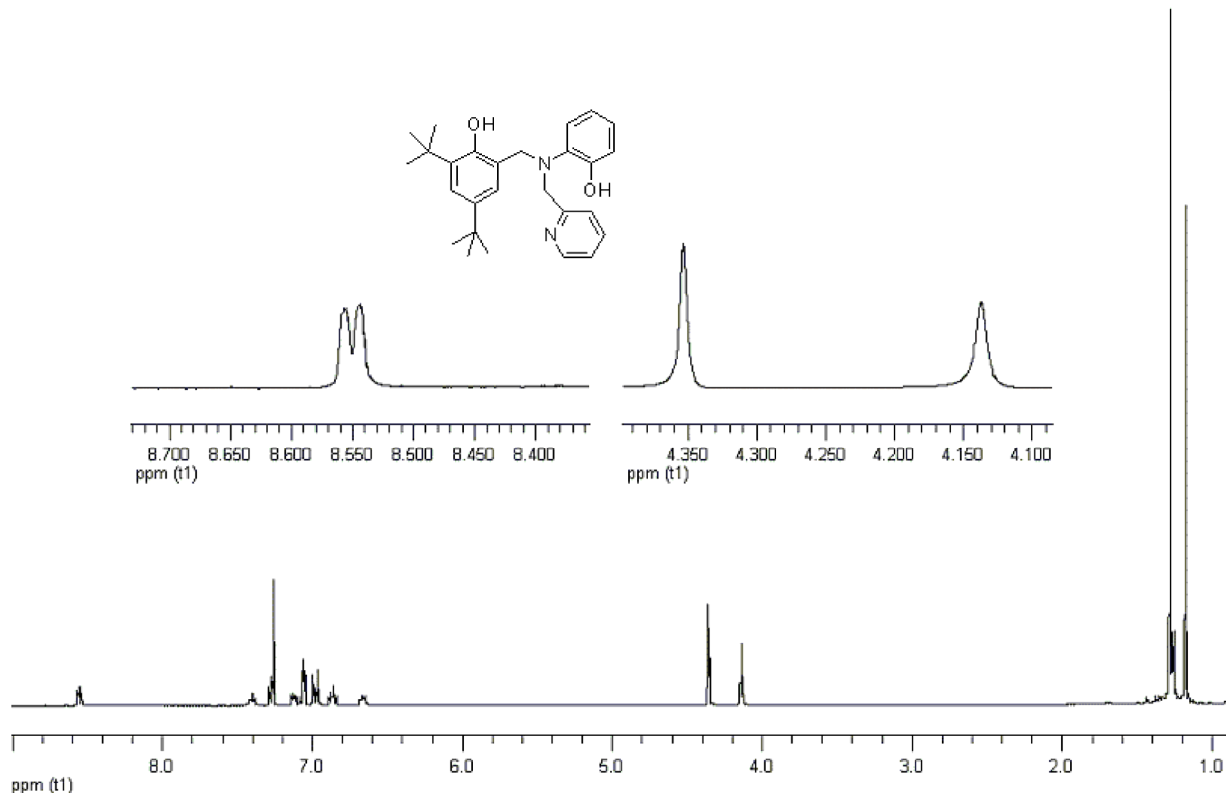


Fig. S1 ^1H NMR spectrum of H_2L in CDCl_3 .

1.2 Spectroscopic characterization of complex L₂Zr (**1**)

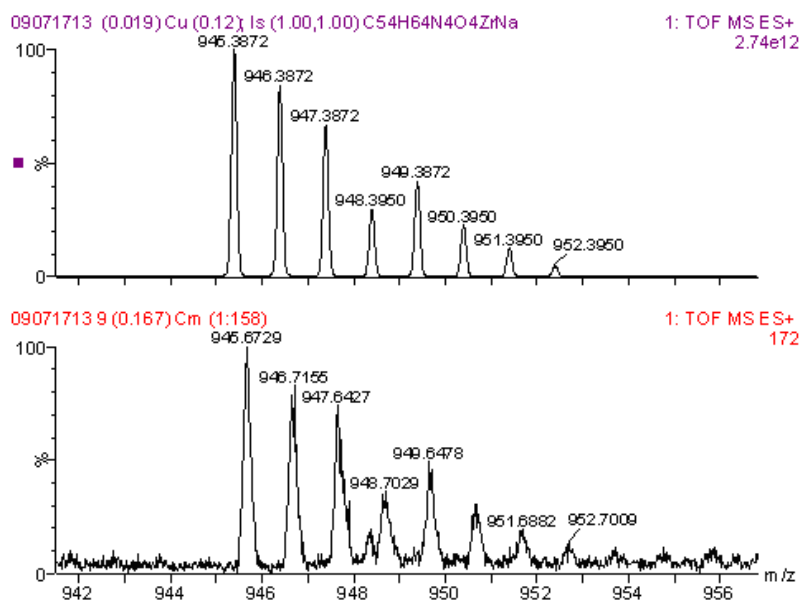


Fig. S2 The calculated (top) and observed (bottom) positive-ion ESI-Q-TOF mass spectra of **1** ([M + Na]⁺) in CH₂Cl₂/acetone.

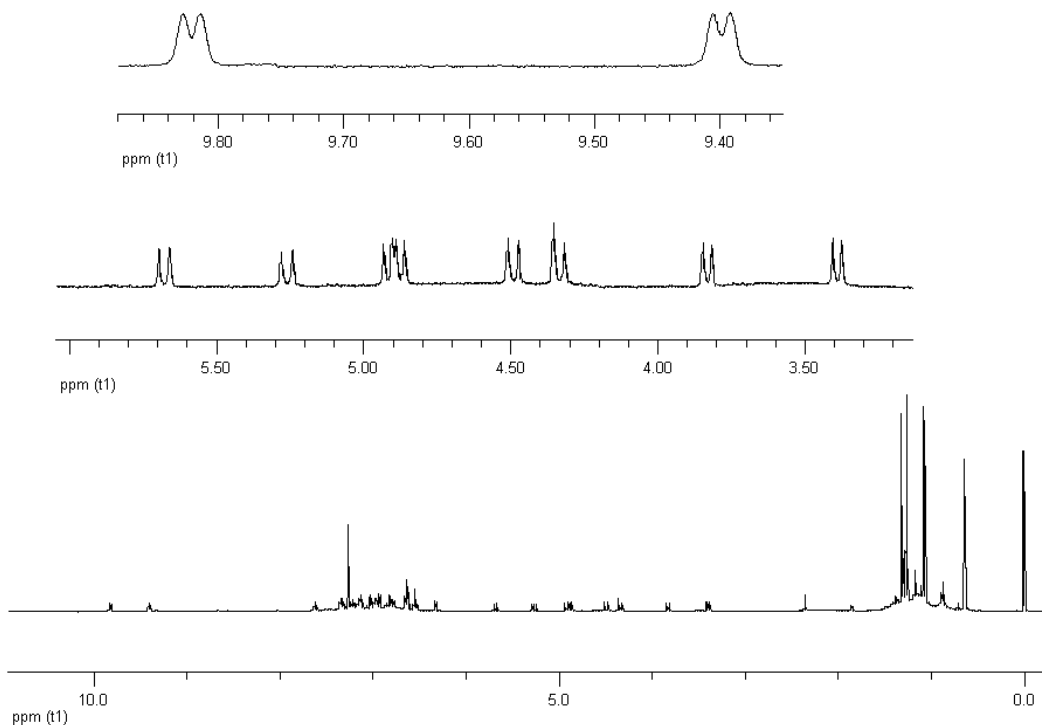


Fig. S3 ¹H NMR spectrum of **1** in CDCl₃.

1.3 ^1H NMR and mass spectra of complexes 2 and 3

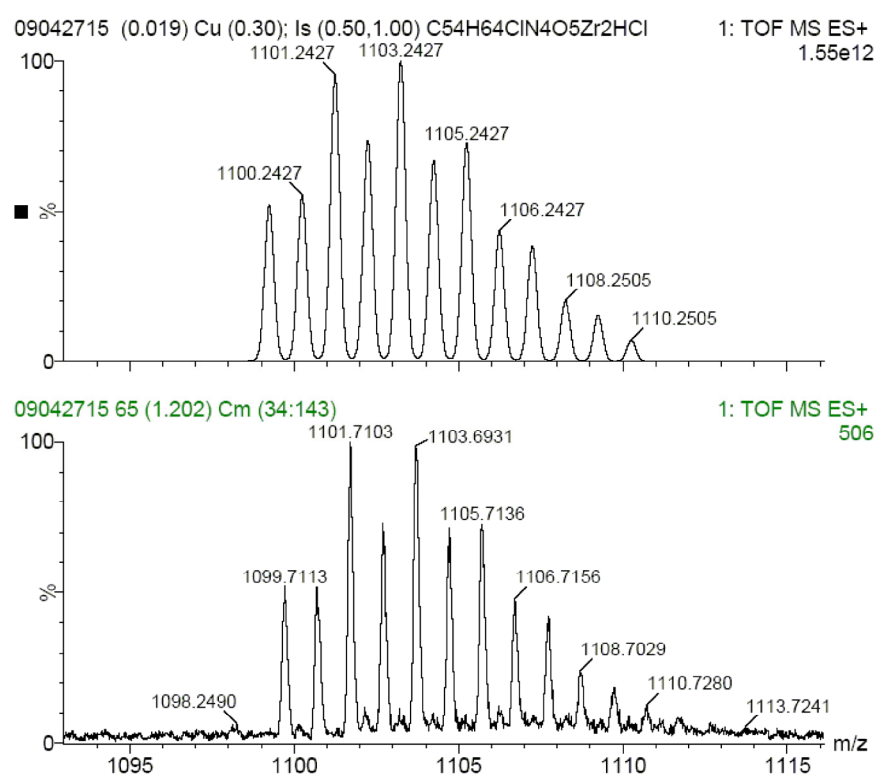


Fig. S4 The calculated (top) and observed (bottom) positive-ion ESI-Q-TOF mass spectra of **2** ($[\text{M}-\text{Cl}]^+$) in $\text{CH}_2\text{Cl}_2/\text{acetone}$.

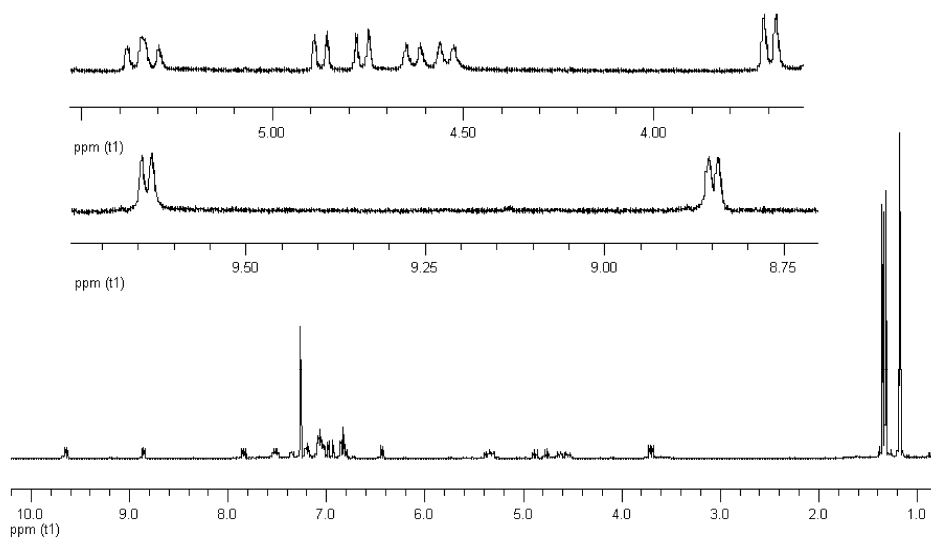


Fig. S5 ^1H NMR spectrum of **2** in CDCl_3 .

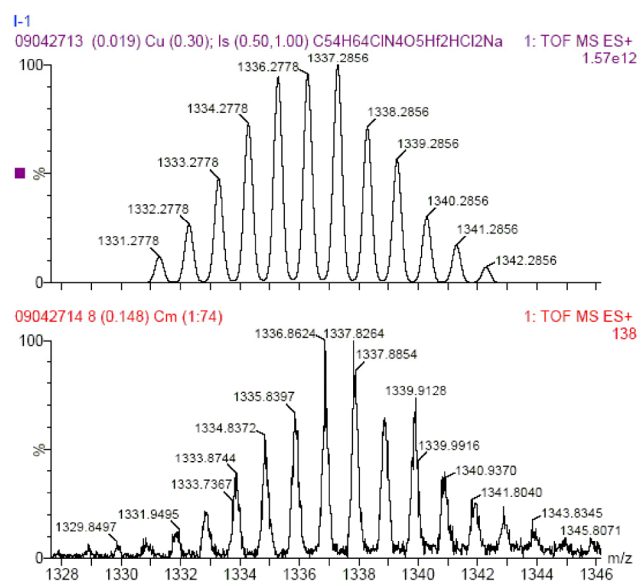


Fig. S6 The calculated (top) and observed (bottom) positive-ion ESI-Q-TOF mass spectra of **3** ($[M+Na]^+$) in $\text{CH}_2\text{Cl}_2/\text{acetone}$.

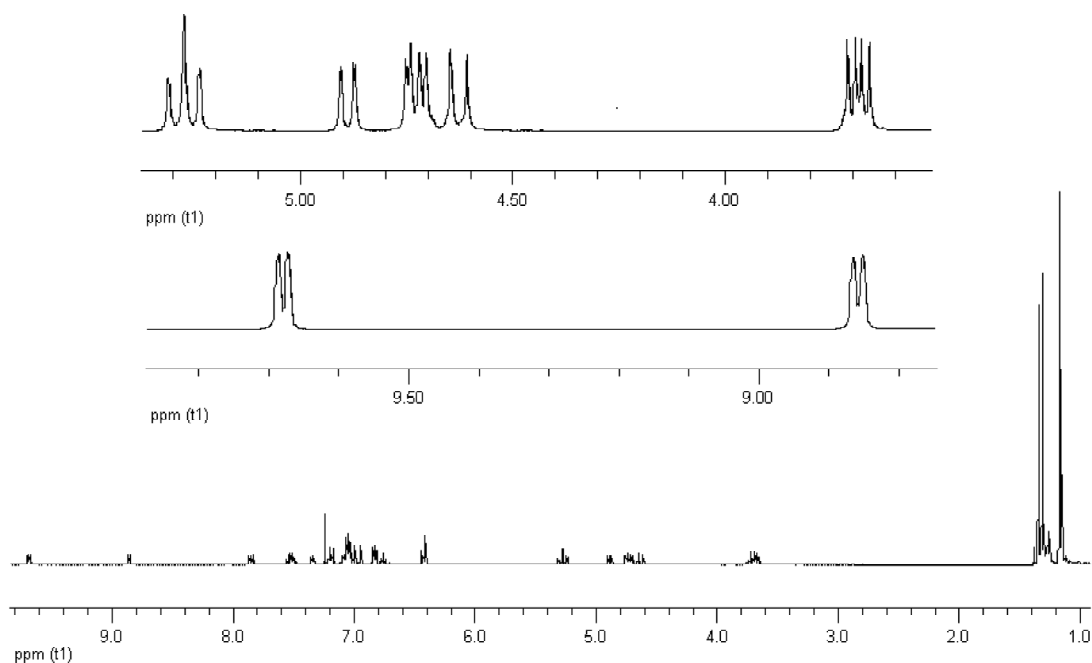


Fig. S7 ¹H NMR spectrum of **3** in CDCl_3 .

1.4 Crystallographic data of H₂L and 1–3

Table S1 Crystallographic data for H₂L and 1

	H ₂ L	L ₂ Zr·0.5C ₆ H ₁₄
Formula	C ₂₇ H ₃₄ N ₂ O ₂	C ₅₄ H ₆₄ N ₄ O ₄ Zr·0.5C ₆ H ₁₄
Formula weight	418.56	967.40
T/K	298(2)	298(2)
Crystal size/mm	0.28 × 0.52 × 0.88	0.16 × 0.21 × 0.28
Crystal system	Orthorhombic	Monoclinic
Space group	Pbca	P2/c
a/Å	10.309(4)	12.6470(15)
b/Å	19.877(7)	20.723(3)
c/Å	23.543(8)	10.6438(14)
β(°)		110.525(7)
V/Å ³	4824(3)	2612.4(6)
Z	8	2
D _{calc} /g cm ⁻³	1.153	1.230
μ/mm ⁻¹	0.072	0.259
F ₀₀₀	1808	1026
θ Range/deg	2.05–25.50	2.27–25.00
Reflections collected	30162	11462
Independent reflections	4489	4440
R _{int}	0.0738	0.0340
Final R ₁ ^a , wR ₂ ^b [I > 2σ(I)]	0.0641, 0.1204	0.0469, 0.1264
R ₁ , wR ₂ (all data)	0.1676, 0.1411	0.0612, 0.1352
Goodness-of-fit on F ²	1.009	1.058
Residual electron density/e Å ⁻³	0.216, -0.278	1.045, -0.219

1.4.1 Crystallographic data of H₂L

Table S2 Selected bond lengths (Å) and angles (deg) for H₂L

	N1–C6	C18–C24	1.537(4)	C3–C2	1.368(6)
N1–C13	1.430(4)	C18–C24	1.529(4)	C20–C21A	1.479(8)
N1–C7	1.473(4)	C24–C26	1.530(4)	C20–C21B	1.493(11)
O1–C1	1.476(4)	C24–C25	1.538(4)	C20–C23A	1.495(9)
O2–C19	1.362(4)	C24–C27	1.383(4)	C20–C22B	1.518(12)
C19–C14	1.374(3)	C6–C5	1.390(5)	C20–C22A	1.578(7)
C19–C18	1.391(4)	C6–C1	1.390(4)	C20–C23B	1.587(10)
N2–C12	1.334(4)	C13–C14	1.384(4)	C12–C11	1.365(5)
N2–C8	1.337(4)	C14–C15	1.384(4)	C9–C10	1.385(5)
C8–C9	1.337(4)	C16–C15	1.390(4)	C10–C11	1.367(6)
C8–C7	1.373(4)	C16–C17	1.390(4)	C2–C1	1.388(4)
C18–C17	1.399(4)	C16–C20	1.528(4)	C5–C4	1.389(5)
C6–N1–C13	1.334(4)	C16–C20	1.359(6)	C1–C6–N1	117.8(3)
C6–N1–C7	1.337(4)	C3–C4	119.3(3)	N2–C8–C9	122.5(3)
C13–N1–C7	1.391(4)	C5–C6–N1	119.6(3)	N2–C8–C7	115.0(3)
O1–C1–C2	1.374(3)	C13–C14–C19	111.7(3)	C12–N2–C8	112.7(3)
O1–C1–C6	1.337(4)	N1–C13–C14	112.7(3)	N2–C12–C11	117.9(3)
O1–C1–C6	1.334(4)	N1–C13–C14	123.6(3)	N2–C12–C11	123.5(4)

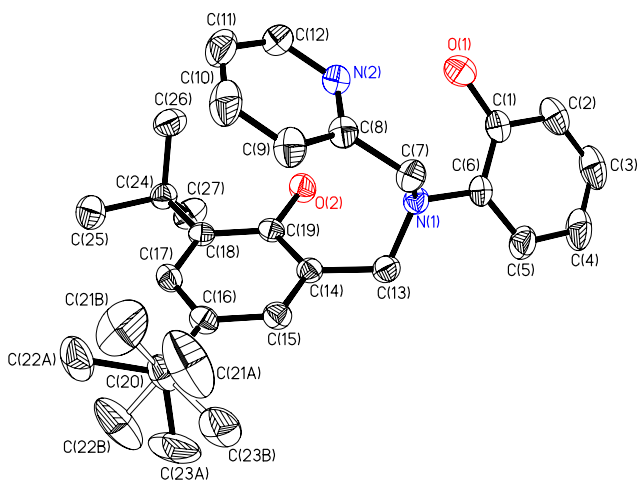


Fig. S8 Molecular structure of H₂L (30% probability ellipsoids). All hydrogen atoms are omitted for clarity.

1.4.2 Crystallographic data of 1

Table S3 Selected bond lengths (\AA) and angles (deg) for **1**

Zr1–O2	2.039(2)	Zr1–O1	2.101(2)	Zr1–N2	2.496(3)
Zr1–N1	2.517(2)				
O2–Zr1–O2A	95.44(11)	O1–Zr1–N2A	70.22(8)	O1–Zr1–N1A	130.36(8)
O2–Zr1–O1	143.93(8)	O2–Zr1–N2	89.00(9)	N2–Zr1–N1A	141.30(8)
O2A–Zr1–O1	84.69(8)	O1–Zr1–N2	72.44(9)	O2–Zr1–N1	72.87(8)
O1–Zr1–O1A	115.72(11)	N2–Zr1–N2A	106.02(13)	O1–Zr1–N1	71.34(8)
O2–Zr1–N2A	145.78(8)	O2–Zr1–N1A	83.12(8)	N2–Zr1–N1	65.80(8)
N1–Zr1–N1A	144.13(11)				

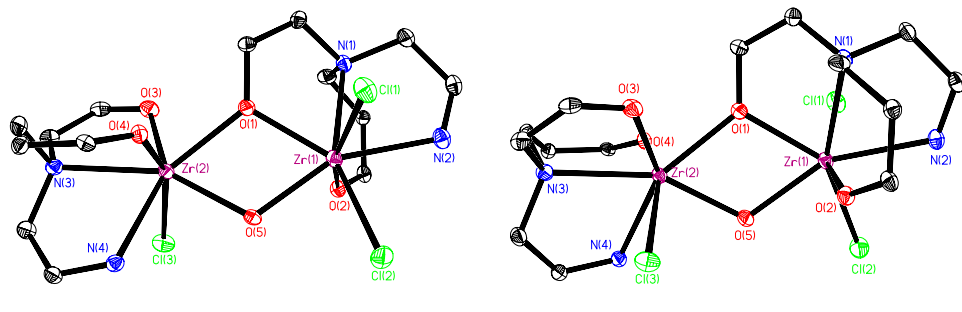
1.4.3 Crystallographic data of N(*R*)N(*R*)-2 and N(*S*)N(*S*)-2

Table S4 Selected bond lengths (\AA) and angles (deg) for N(*R*)N(*R*)-2

Zr1–O2	1.996(3)	Zr1–Cl1	2.4527(11)	Zr2–O1	2.218(3)
Zr1–O5	2.159(3)	Zr1–Cl2	2.5156(11)	Zr2–N4	2.375(3)
Zr1–O1	2.172(3)	Zr2–O4	2.004(3)	Zr2–N3	2.441(3)
Zr1–N2	2.422(3)	Zr2–O3	2.023(2)	Zr2–Cl3	2.5086(11)
Zr1–N1	2.444(3)	Zr2–O5	2.133(2)	Zr2…Zr1	3.6238(6)
O4–Zr2–O3	107.34(11)	N3–Zr2–Cl3	84.42(8)	O1–Zr1–Cl1	85.52(7)
O4–Zr2–O5	100.84(10)	O4–Zr2–Zr1	97.33(7)	N2–Zr1–Cl1	81.04(8)
O3–Zr2–O5	130.21(10)	O3–Zr2–Zr1	102.50(8)	N1–Zr1–Cl1	83.16(8)
O4–Zr2–O1	83.56(10)	O5–Zr2–Zr1	32.61(7)	O2–Zr1–Cl2	98.12(8)
O3–Zr2–O1	77.26(10)	O1–Zr2–Zr1	33.96(6)	O5–Zr1–Cl2	76.83(7)
O5–Zr2–O1	65.97(9)	N4–Zr2–Zr1	116.53(8)	O1–Zr1–Cl2	136.50(7)
O4–Zr2–N4	79.54(11)	N3–Zr2–Zr1	173.31(7)	N2–Zr1–Cl2	83.45(9)
O3–Zr2–N4	139.38(11)	Cl3–Zr2–Zr1	99.36(3)	N1–Zr1–Cl2	152.60(8)
O5–Zr2–N4	85.09(10)	O2–Zr1–O5	88.58(10)	Cl1–Zr1–Cl2	88.61(4)
O1–Zr2–N4	142.92(10)	O2–Zr1–O1	103.11(10)	O2–Zr1–Zr2	92.00(8)
O4–Zr2–N3	80.93(10)	O5–Zr1–O1	66.35(9)	O5–Zr1–Zr2	32.18(6)
O3–Zr2–N3	72.07(11)	O2–Zr1–N2	79.10(11)	O1–Zr1–Zr2	34.77(7)
O5–Zr2–N3	154.02(10)	O5–Zr1–N2	155.02(11)	N2–Zr1–Zr2	166.55(8)
O1–Zr2–N3	139.4(1)	O1–Zr1–N2	137.49(11)	N1–Zr1–Zr2	99.40(8)
N4–Zr2–N3	69.63(11)	O2–Zr1–N1	81.37(10)	Cl1–Zr1–Zr2	105.76(3)
O4–Zr2–Cl3	155.18(8)	O5–Zr1–N1	130.36(10)	Cl2–Zr1–Zr2	107.99(3)
O3–Zr2–Cl3	86.81(8)	O1–Zr1–N1	68.97(10)	Zr2–O5–Zr1	115.20(11)
O5–Zr2–Cl3	83.95(7)	N2–Zr1–N1	69.49(11)	Zr1–O1–Zr2	111.27(10)
O1–Zr2–Cl3	120.06(7)	O2–Zr1–Cl1	158.12(8)		
N4–Zr2–Cl3	76.61(8)	O5–Zr1–Cl1	113.26(7)		

Table S5 Selected bond lengths (\AA) and angles (deg) for $\text{N}(S)\text{N}(S)\text{-2}$

Zr1–O2	1.997(2)	Zr1–Cl1	2.4540(8)	Zr2–O1	2.2142(18)
Zr1–O5	2.1569(19)	Zr1–Cl2	2.5155(8)	Zr2–N4	2.377(2)
Zr1–O1	2.170(2)	Zr2–O4	2.001(2)	Zr2–N3	2.448(2)
Zr1–N2	2.418(2)	Zr2–O3	2.0232(19)	Zr2–Cl3	2.5104(9)
Zr1–N1	2.446(2)	Zr2–O5	2.1325(19)	Zr2–Zr1	3.6236(4)
O4–Zr2–O3	107.44(9)	N3–Zr2–Cl3	84.45(6)	O1–Zr1–Cl1	85.64(6)
O4–Zr2–O5	101.10(8)	O4–Zr2–Zr1	97.51(6)	N2–Zr1–Cl1	81.12(7)
O3–Zr2–O5	130.14(8)	O3–Zr2–Zr1	102.62(6)	N1–Zr1–Cl1	83.11(6)
O4–Zr2–O1	83.82(8)	O5–Zr2–Zr1	32.56(5)	O2–Zr1–Cl2	98.19(6)
O3–Zr2–O1	77.45(7)	O1–Zr2–Zr1	33.88(5)	O5–Zr1–Cl2	76.96(5)
O5–Zr2–O1	65.87(7)	N4–Zr2–Zr1	116.46(6)	O1–Zr1–Cl2	136.58(5)
O4–Zr2–N4	79.47(8)	N3–Zr2–Zr1	173.39(6)	N2–Zr1–Cl2	83.31(6)
O3–Zr2–N4	139.28(8)	Cl3–Zr2–Zr1	99.36(2)	N1–Zr1–Cl2	152.47(6)
O5–Zr2–N4	85.10(8)	O2–Zr1–O5	88.58(8)	Cl1–Zr1–Cl2	88.56(3)
O1–Zr2–N4	142.87(8)	O2–Zr1–O1	102.94(8)	O2–Zr1–Zr2	92.03(6)
O4–Zr2–N3	80.68(8)	O5–Zr1–O1	66.23(7)	O5–Zr1–Zr2	32.15(5)
O3–Zr2–N3	72.08(8)	O2–Zr1–N2	79.06(8)	O1–Zr1–Zr2	34.66(5)
O5–Zr2–N3	153.99(8)	O5–Zr1–N2	154.97(8)	N2–Zr1–Zr2	166.60(6)
O1–Zr2–N3	139.55(8)	O1–Zr1–N2	137.62(8)	N1–Zr1–Zr2	99.46(6)
N4–Zr2–N3	69.59(8)	O2–Zr1–N1	81.37(8)	Cl1–Zr1–Zr2	105.68(2)
O4–Zr2–Cl3	155.05(6)	O5–Zr1–N1	130.37(8)	Cl2–Zr1–Zr2	108.06(2)
O3–Zr2–Cl3	86.63(7)	O1–Zr1–N1	69.03(8)	Zr2–O5–Zr1	115.29(9)
O5–Zr2–Cl3	83.87(6)	N2–Zr1–N1	69.51(8)	Zr1–O1–Zr2	111.47(8)
O1–Zr2–Cl3	119.95(6)	O2–Zr1–Cl1	158.13(6)		
N4–Zr2–Cl3	76.60(6)	O5–Zr1–Cl1	113.25(6)		



$\text{N}(R)\text{N}(R)\text{-2}$

$\text{N}(S)\text{N}(S)\text{-2}$

Fig. S9 Framework structures of $\text{N}(R)\text{N}(R)\text{-2}$ and $\text{N}(S)\text{N}(S)\text{-2}$ (30% probability ellipsoids).

Parts of the phenyl and pyridyl rings are omitted for clarity.

1.4.4 Crystallographic data of N(R)N(R)-3 and N(S)N(S)-3

Two enantiomers were identified for complex **3**, that is, N(S)N(S)-**3** and N(R)N(R)-**3** (Table S6 and S7)

Table S6 Selected bond lengths (\AA) and angles (deg) for N(R)N(R)-**3**

Hf1–O2	1.999(6)	Hf1–Cl1	2.437(3)	Hf2–O1	2.211(5)
Hf1–O5	2.117(6)	Hf1–Cl2	2.487(2)	Hf2–N4	2.375(6)
Hf1–O1	2.158(6)	Hf2–O4	1.968(6)	Hf2–N3	2.382(7)
Hf1–N2	2.385(8)	Hf2–O3	2.018(6)	Hf2–Cl3	2.482(2)
Hf1–N1	2.434(7)	Hf2–O5	2.119(5)	Hf2…Hf1	3.5960(6)
O4–Hf2–O3	106.0(2)	N3–Hf2–Cl3	84.34(17)	O1–Hf1–Cl1	85.55(17)
O4–Hf2–O5	100.3(2)	O4–Hf2–Hf1	97.26(16)	N2–Hf1–Cl1	83.1(2)
O3–Hf2–O5	130.1(2)	O3–Hf2–Hf1	102.25(19)	N1–Hf1–Cl1	82.4(2)
O4–Hf2–O1	82.9(2)	O5–Hf2–Hf1	31.89(15)	O2–Hf1–Cl2	98.77(17)
O3–Hf2–O1	76.7(2)	O1–Hf2–Hf1	34.14(15)	O5–Hf1–Cl2	77.53(17)
O5–Hf2–O1	65.3(2)	N4–Hf2–Hf1	115.48(18)	O1–Hf1–Cl2	137.10(15)
O4–Hf2–N4	80.8(2)	N3–Hf2–Hf1	174.45(17)	N2–Hf1–Cl2	83.1(2)
O3–Hf2–N4	140.7(3)	Cl3–Hf2–Hf1	97.89(6)	N1–Hf1–Cl2	151.8(2)
O5–Hf2–N4	84.5(2)	O2–Hf1–O5	87.0(2)	Cl1–Hf1–Cl2	88.41(11)
O1–Hf2–N4	142.3(2)	O2–Hf1–O1	101.4(2)	O2–Hf1–Hf2	89.36(17)
O4–Hf2–N3	82.2(2)	O5–Hf1–O1	66.2(2)	O5–Hf1–Hf2	31.92(15)
O3–Hf2–N3	72.7(3)	O2–Hf1–N2	79.0(3)	O1–Hf1–Hf2	35.08(14)
O5–Hf2–N3	153.7(2)	O5–Hf1–N2	154.0(3)	N2–Hf1–Hf2	164.75(19)
O1–Hf2–N3	140.5(2)	O1–Hf1–N2	137.8(3)	N1–Hf1–Hf2	99.55(19)
N4–Hf2–N3	69.9(2)	O2–Hf1–N1	82.5(2)	Cl1–Hf1–Hf2	106.36(7)
O4–Hf2–Cl3	157.26(16)	O5–Hf1–N1	130.5(2)	Cl2–Hf1–Hf2	108.61(6)
O3–Hf2–Cl3	87.21(19)	O1–Hf1–N1	68.8(2)	Hf1–O5–Hf2	116.2(3)
O5–Hf2–Cl3	84.08(17)	N2–Hf1–N1	69.4(3)	Hf1–O1–Hf2	110.8(2)
O1–Hf2–Cl3	118.64(16)	O2–Hf1–Cl1	159.75(18)		
N4–Hf2–Cl3	77.42(19)	O5–Hf1–Cl1	113.15(17)		

Table S7 Selected bond lengths (\AA) and angles (deg) for N(S)N(S)-**3**

Hf1–O2	1.999(4)	Hf1–Cl1	2.4437(17)	Hf2–O1	2.206(3)
Hf1–O5	2.131(3)	Hf1–Cl2	2.4878(16)	Hf2–N4	2.361(4)
Hf1–O1	2.162(4)	Hf2–O4	1.990(4)	Hf2–N3	2.412(4)
Hf1–N2	2.400(5)	Hf2–O3	2.027(3)	Hf2–Cl3	2.4878(15)
Hf1–N1	2.424(4)	Hf2–O5	2.114(3)	Hf2…Hf1	3.5998(3)
O4–Hf2–O3	106.12(17)	N3–Hf2–Cl3	84.35(12)	O1–Hf1–Cl1	85.95(11)
O4–Hf2–O5	100.36(14)	O4–Hf2–Hf1	97.41(8)	N2–Hf1–Cl1	83.35(14)
O3–Hf2–O5	130.42(16)	O3–Hf2–Hf1	102.37(11)	N1–Hf1–Cl1	82.59(12)
O4–Hf2–O1	83.19(13)	O5–Hf2–Hf1	32.16(9)	O2–Hf1–Cl2	98.58(11)
O3–Hf2–O1	76.83(13)	O1–Hf2–Hf1	34.11(10)	O5–Hf1–Cl2	77.55(10)
O5–Hf2–O1	65.52(13)	N4–Hf2–Hf1	115.89(10)	O1–Hf1–Cl2	137.09(10)
O4–Hf2–N4	79.96(15)	N3–Hf2–Hf1	174.49(10)	N2–Hf1–Cl2	82.86(13)
O3–Hf2–N4	140.33(13)	Cl3–Hf2–Hf1	97.85(4)	N1–Hf1–Cl2	151.90(11)
O5–Hf2–N4	84.71(14)	O2–Hf1–O5	87.26(14)	Cl1–Hf1–Cl2	88.39(7)
O1–Hf2–N4	142.33(13)	O2–Hf1–O1	101.42(14)	O2–Hf1–Hf2	89.62(9)
O4–Hf2–N3	82.03(14)	O5–Hf1–O1	66.02(12)	O5–Hf1–Hf2	31.86(9)
O3–Hf2–N3	72.63(15)	O2–Hf1–N2	78.38(16)	O1–Hf1–Hf2	34.91(8)
O5–Hf2–N3	153.35(13)	O5–Hf1–N2	153.66(17)	N2–Hf1–Hf2	164.68(11)
O1–Hf2–N3	140.61(14)	O1–Hf1–N2	138.24(15)	N1–Hf1–Hf2	99.49(11)
N4–Hf2–N3	69.47(14)	O2–Hf1–N1	82.25(16)	Cl1–Hf1–Hf2	106.57(4)
O4–Hf2–Cl3	157.14(9)	O5–Hf1–N1	130.41(14)	Cl2–Hf1–Hf2	108.60(4)
O3–Hf2–Cl3	87.05(13)	O1–Hf1–N1	68.91(14)	Hf2–O5–Hf1	115.98(16)
O5–Hf2–Cl3	83.97(11)	N2–Hf1–N1	69.72(17)	Hf1–O1–Hf2	110.98(15)
O1–Hf2–Cl3	118.52(11)	O2–Hf1–Cl1	159.41(10)		
N4–Hf2–Cl3	78.10(13)	O5–Hf1–Cl1	113.22(11)		

2. Studies on polymerization of lactide using racemic initiators **2** and **3**

2.1 Typical procedure for polymerization of *rac*-LA

The stereoselectivities of the PLA are determined by the homonuclear decoupled ^1H NMR spectra of the methine region of the products (Fig. S10).

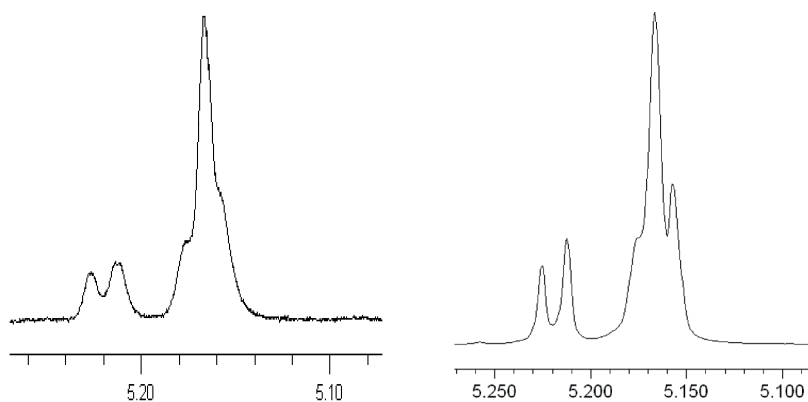


Fig. S10 Methine region of homonuclear decoupled ^1H NMR spectra of isotactic-rich PLA made from *rac*-LA initiated by *rac*-**2** (CDCl_3 , 400 MHz, left) and *rac*-**3** (CDCl_3 , 600 MHz, right).

2.2 Polymerization of L-LA and microstructure analysis of PLLA

Polymerization of L-LA was made by the same procedure as that for *rac*-LA. The tacticity of the polymers prepared with the racemic initiator **2** was determined by inspection of the homonuclear decoupled ^1H NMR spectrum of the methine region. (Fig. S11).

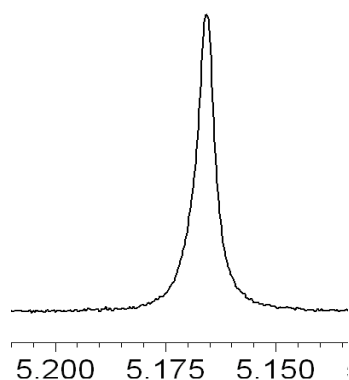


Fig. S11 Homonuclear decoupled ^1H NMR spectrum of the methine region of PLLA prepared from L-LA with the racemic initiator **2** at 130 °C (400 MHz, CDCl_3).